NASA MEMO 2-20-59A

NASA

MEMORANDUM

FULL-SCALE WIND-TUNNEL INVESTIGATION OF A JET FLAP IN CONJUNCTION WITH A PLAIN FLAP WITH BLOWING BOUNDARY-LAYER CONTROL ON A 35° SWEPTBACK-WING AIRPLANE

By Kiyoshi Aoyagi and David H. Hickey

Ames Research Center
Moffett Field, Calif.

NATIONAL AERONAUTICS AND SPACE ADMINISTRATION
WASHINGTON
March 1959

NATIONAL AERONAUTICS AND SPACE ADMINISTRATION

MEMORANDUM 2-20-59A

FULL-SCALE WIND-TUNNEL INVESTIGATION OF A JET FLAP IN CONJUNCTION WITH A PLAIN FLAP WITH BLOWING BOUNDARY-LAYER CONTROL ON A 35° SWEPTBACK-WING AIRPLANE

By Kiyoshi Aoyagi and David H. Hickey

SUMMARY

Previous investigations have shown that increased blowing at the hinge-line radius of a plain flap will give flap lift increases above that realized with boundary-layer control. Other experiments and theory have shown that blowing from a wing trailing edge, through the jet flap effect, produced lift increases. The present investigation was made to determine whether blowing simultaneously at the hinge-line radius and trailing edge would be more effective than blowing separately at either location. The tests were made at a Reynolds number of 4.5×10^6, with a 35° sweptback-wing airplane. For this report, only the lift data are presented.

Of the three flap blowing arrangements tested, blowing distributed between the trailing edge and the hinge-line radius of a plain flap was found to be superior to blowing at either location separately at the plain flap deflections of interest.

Comparison of estimated and experimental jet flap effectiveness was fair.

INTRODUCTION

As part of the 40- by 80-foot wind tunnel tests of high-lift aids at low speed, the use of blowing boundary-layer control on the trailing-edge flaps has been investigated. References 1 and 2 have shown an increase of lift coefficient with blowing-jet momentum coefficient. Although the rate of lift-coefficient increase with momentum coefficient was less than that prior to flow attachment, the lift-coefficient increase after flow attachment was still greater than that of the reaction component of the jet momentum. Working in the high momentum coefficient range, several investigators (refs. 3 and 4) have proposed using a jet flap as a high-lift device. The jet flap increases the circulation about the wing by ejecting a high velocity jet of air downward from the wing trailing

edge. At the low momentum coefficient range (C_μ less than 1.0), however, the jet flap is an inefficient lift generator when compared to a trailing-edge flap with blowing boundary-layer control (ref. 5).

The present investigation was undertaken on an airplane with a 35° sweptback wing with aspect ratio of 4.94 and taper ratio of 0.5 to determine if the combination of the jet flap and a plain trailing-edge flap with blowing boundary-layer control at the flap radius would be more effective as a lift generator than either device separately. The emphasis of this report is on lift and its variation with momentum coefficient. Although drag and pitching-moment data were obtained, the thrust data corrections were so large because of the low tunnel speed at which the test was conducted that it was impossible to draw reliable conclusions regarding the effect of various flap arrangements on these characteristics. The tests were conducted at a Reynolds number of 4.5×10^6 and covered a range of momentum coefficients from 0 to 0.24. A comparison of experimental results with theoretical results derived from two-dimensional theory is also included.

NOTATION

b wing span, ft

BLC boundary-layer control

c wing chord parallel to plane of symmetry, ft

c_f flap chord parallel to plane of symmetry, ft

c_l two-dimensional lift coefficient, $\frac{\text{lift per unit span}}{q_\infty c}$

c_μ two-dimensional momentum coefficient, $\frac{w_j/g}{q_\infty c} V_j$

$\bar{c}$ mean aerodynamic chord, $\frac{2}{S}\int_0^{b/2} c^2 dy$, ft

C_L lift coefficient, $\frac{\text{lift}}{q_\infty S}$

ΔC_L lift-coefficient increment

C_μ momentum coefficient, $\frac{W_j/g}{q_\infty S} V_j$

$C_{L_{\underline{\delta}_1}}$ variation of lift coefficient with flap deflection, per radian, for $\frac{c_f}{c} = 1$

$\frac{d\alpha}{d\delta}$ two-dimensional flap lift-effectiveness parameter

F_G gross thrust from engine, lb

g acceleration of gravity, 32.2 ft/sec^2

q dynamic pressure, lb/sq ft

S wing area, sq ft

S_f wing area spanned by flaps, sq ft

V_j jet velocity assuming isentropic expansion, ft/sec

W weight rate of flow, lb/sec

w_j weight rate of flow per unit span, lb/sec

x distance along airfoil chord normal to wing quarter-chord line, in.

z height above wing reference plane defined by quarter-chord line and chord of the wing section at $0.663 \frac{b}{2}$, in.

Λ sweep angle, deg

α angle of attack of fuselage reference line, deg

δ_f flap deflection, measured normal to flap hinge line (given as $\underline{\delta}$ in ref. 9), deg

$\underline{\delta}_f$ flap deflection measured parallel to the plane of symmetry (given as δ in ref. 9), deg

δ_j angle of trailing-edge jet, measured normal to the trailing edge, deg

$\underline{\delta}_j$ angle of trailing-edge jet, measured parallel to the plane of symmetry, deg

Subscripts

f	flap
j	jet
te	trailing edge
u	uncorrected
∞	free stream

MODEL AND APPARATUS

Figure 1 is a photograph of the model mounted in the Ames 40- by 80-foot wind tunnel. The model tested is the same as that reported in reference 2. Major dimensions of aerodynamic importance are shown in figure 2.

Wing

Plan form and airfoil sections.- The wing had a quarter-chord sweep of 35°, aspect ratio of 4.94, and a taper ratio of 0.50. Airfoil sections normal to the wing quarter-chord line were modified NACA 0012-64 and 0011-64 sections at the root and tip, respectively. Coordinates of the airfoil sections at two semispan stations are given in table I.

Flap and nozzles.- Details of the wing and flap are shown in figure 3. The blowing BLC flap of reference 2 was replaced with a flap equipped with blowing nozzles located both at the flap radius and at the trailing edge. Chordwise location of the nozzle at the flap radius as shown in figure 3 was used throughout the tests. High-pressure air for blowing entered at the root and thence into the hollow flap which acted as a plenum chamber for both nozzles.

Engine and Ducting

A J-57 turbojet engine was installed in the airplane to provide high-pressure air to the jet flap and for BLC. Air was bled off the high-pressure compressor stage of the engine, and the flow was regulated by valves located at each flap duct.

Instrumentation

Measurements to obtain the momentum coefficient.- Weight rate of flow to each flap was obtained by measurement of total and static pressure and temperature in the duct leading to each flap. These same total pressure and temperature measurements were used to compute C_μ. Because there was no provision to determine C_μ values at the flap radius and trailing-edge nozzles separately, relative C_μ values at each nozzle location were determined by the ratio of the nozzle areas.

Measurement of thrust.- The gross thrust of the engine was obtained in the same manner as described in reference 2.

TESTS

Range of Variables

Momentum coefficient.- The investigation covered a range of momentum coefficients from 0 to 0.24 and flap jet pressure ratios from subcritical to approximately 5.8. All tests were made with the horizontal tail off at a Reynolds number of 4.5×10^6, based on the mean aerodynamic chord of 8.22 feet. This Reynolds number corresponds to a free-stream dynamic pressure of 10 pounds per square foot.

Nozzle height.- When total blowing was employed either at the plain flap radius or trailing edge, the nozzle heights were 0.045 and 0.030 inch, respectively. When a jet flap combined with a plain flap with BLC was tested, that is, blowing at both the trailing edge and flap radius, a nozzle height of, respectively, 0.030 and 0.010 inch was used. The relative weight rate of air flow and relative momentum coefficient values with the above nozzle openings were approximately 75 percent and 25 percent, respectively, of the total weight rate of air flow and total momentum coefficient.

Plain flap deflection.- The model was tested with the jet flap combined with the plain flap deflected 0°, 30°, and 45°. Tests were made with BLC over the flap radius at flap deflections of 30°, 45°, and 60° with and without the jet flap.

Jet flap angle.- Jet flap angles tested were 0°, 45°, and 90° measured with respect to the flap chord line. The jet flap angles discussed in this report will be referred with respect to the flap chord line regardless of the plain flap deflection.

Method of Testing

Lift.- The major portion of the data were obtained by varying momentum coefficient at 0° angle of attack for the jet flap, plain flap, or the jet flap combined with BLC on the plain flap. In addition, data were obtained through the angle-of-attack range with fixed values of momentum coefficient.

Engine thrust calibration.- The gross thrust of the engine was computed as described in reference 2.

CORRECTIONS

Effects of Wind-Tunnel Walls

The following correction for the effect of wind-tunnel wall interference was made:

$$\alpha = \alpha_u + 0.639\ C_L$$

Effects of Engine Operation

Lift data obtained from the wind-tunnel balance system were corrected for effects of engine thrust as follows:

$$C_L = \frac{\text{total lift}}{q_\infty S} - \frac{F_G}{q_\infty S} \sin \alpha$$

RESULTS AND DISCUSSION

Variation of Lift With Momentum Coefficient at 0° Angle of Attack

The variation of C_L with C_μ with the jet flap at several plain flap deflections is shown in figure 4. The jet flap is defined in this report as a high-velocity air jet located at the trailing edge of the plain flap and ejected at an angle δ_j to the chord line of the plain flap whether the latter is deflected or not.

Jet flap at $\delta_f = 0°$.- A major part of the lift obtained from the jet flap without the plain flap deflected was realized when the jet was deflected 45° as shown in figure 4(a). For this model, little gain was realized by increasing jet deflection to 90°. This finding is supported

by trends shown in the two-dimensional data presented in reference 4. Data from reference 6 for an unswept, untapered wing with full-span jet flap, with the nozzle located on the upper surface, and with a trailing-edge radius that was much larger than either that of the subject model or the model of reference 4 showed increasing lift increments up to $\delta_j = 86^\circ$. It appears possible, therefore, that the subject model was limited in lift because of the poor (from a jet flap effectiveness standpoint) trailing-edge configuration.

Jet flap combined with plain flap.- Without trailing-edge blowing, the plain flap deflected 30° has near theoretical lift as shown in figure 4(a). Applying trailing-edge blowing gave lift-increment increases similar to that obtained from the jet flap with the plain flap undeflected except at $\delta_j = 0^\circ$. Although the lift due to momentum coefficient is similar, the lift due to the plain flap is maintained, giving a substantial ΔC_L compared to the jet flap throughout the momentum coefficient range tested. As was true with the jet flap, lift increments due to momentum coefficient were greater for the jet deflected 45° and 90° than for 0°, and lift increments with 45° and 90° deflection were almost equal.

Data with the plain flap deflected 45° were obtained only for the jet flap deflected 45° (fig. 4(a)). With no blowing at the trailing edge, the plain flap lift increment was below the theoretical value, indicating a condition of flow separation at the plain flap radius. Because of this condition, the lift with trailing-edge blowing was considerably less than the expected values for a 45° flap deflection.

Jet flap with BLC plain flap.- The variation of lift with momentum coefficient for the combination of the jet flap and several deflections of the plain flap with BLC is shown in figure 4(b). The jet flap deflected 45° gave the highest values of C_L at any momentum coefficient for all three plain flap deflections. With the jet flap deflected 45° the lift differences between the three plain flap deflections at higher C_μ values are approximately equal to the difference in theoretical lifts for the three deflections without a jet flap.

The approximate effect of BLC on the plain flap combined with the jet flap is shown in figure 4(c). For the case of the jet flap with BLC plain flap, momentum coefficient at the trailing edge was determined by taking 75 percent of total momentum coefficient values shown in figure 4(b). As would be expected, the plain flap deflected 30° showed little effect of BLC. With the flap deflected 45°, the effect of BLC was substantial at low momentum coefficient values. However, at the high momentum coefficient values, the effect of BLC was diminished since lifts were nearly identical with or without blowing at the plain flap radius.

Comparison of lift with total blowing at the plain flap radius, total blowing at the trailing edge, and blowing distributed between the two locations.- Figure 4(d) presents data showing the best jet flap configurations for the three plain flap deflections from figures 4(a) and (b) and data obtained with total blowing at the plain flap hinge-line radius. With the plain flap deflected 30°, the jet flap gave the highest increase in lift of the three flap blowing arrangements tested. With the plain flap deflected 45°, the divided blowing system was better at the low values of momentum coefficient because of the need for boundary-layer control; but at the high values of momentum coefficient, the jet flap was just as effective as the divided blowing system. With the plain flap deflected 60°, the divided blowing system was better than blowing entirely at the plain flap radius. The gain in lift, however, was small. No data were obtained with the jet flap at 60° of plain flap deflection.

The lift increment due to blowing distributed between the jet flap and the plain flap radius was large at 30° of plain flap deflection and decreased to a small value at 60° of flap deflection when compared to that obtained with total blowing at the plain flap radius.

Effect of Angle of Attack

The foregoing discussion (at $\alpha_u = 0°$) would also be applicable at other angles of attack less than $C_{L_{max}}$ as shown by the typical results in figure 5.

Comparison of Calculated and Experimental Jet Flap Effectiveness

References 7 and 8 present a rheoelectric analogy solution of theory for an airfoil with blowing. Two-dimensional solutions for several blowing methods are included. These results have been used with adjustments for finite aspect ratio and partial span plain flap calculated from reference 9. Details of the method used to calculate ΔC_L are outlined in the appendix. Calculated estimates are compared with experimental data in figure 6.

Jet flap with plain flap undeflected.- Agreement between experimental and calculated results range from good at low momentum coefficient values to fair at high values with the jet flap deflected 45°. At a momentum coefficient of 0.14, the highest value tested, the calculated result is about 70 percent of the experimental ΔC_L.

Jet flap ($\delta_j = 45^o$) with plain flap deflected.- With the plain flap at 30^o, both theory and experiment show the same lift with no blowing, but theory shows lower lift increments with momentum coefficient than experimental results.

Since separated flow occurred initially over the plain flap radius with the plain flap deflected 45^o, experiment shows a flap lift increment well below theory with no blowing. At the higher C_μ values, there is good agreement with theory. It would be necessary to limit BLC to that required to establish flow attachment throughout the jet momentum range over the plain flap radius in order to make a completely valid comparison. This was not possible with the subject model because of the ducting arrangement.

In summary, for the subject wing, the calculated lift increments due to blowing, based on the method outlined in the appendix with the jet flap deflected 45^o, give fair agreement with what was found experimentally with the plain flap undeflected and good agreement with the plain flap deflected 30^o. Agreement was good only at high momentum coefficient values with the plain and jet flaps deflected 45^o.

CONCLUSIONS

For equivalent values of momentum coefficient and at the plain flap deflections of interest, blowing at the trailing edge and at the hinge-line radius of a plain flap produced values of lift greater than could be realized by blowing separately at either location. At the low plain flap deflection, the combination of jet flap and plain flap with boundary-layer control provided a large increase in lift increment, but at the high flap deflection, the increase over that obtained with blowing entirely at the plain flap radius was small. When compared to the combination of jet flap and plain flap without BLC, the addition of boundary-layer control on the plain flap to the jet flap increased lift at low values of momentum coefficient but made little change at high values of momentum coefficient.

Comparison of theoretical and experimental jet flap effectiveness at a jet angle of 45^o ranged from fair to good depending upon the momentum coefficient.

Ames Research Center
National Aeronautics and Space Administration
Moffett Field, Calif., Nov. 20, 1958

APPENDIX

THEORETICAL COMPUTATION OF JET FLAP EFFECTIVENESS

Reference 7 presents two-dimensional solutions of blowing airfoil theory. Lift coefficient with any combination of jet flap or plain flap can be calculated. Two-dimensional circulation lift is expressed as follows:

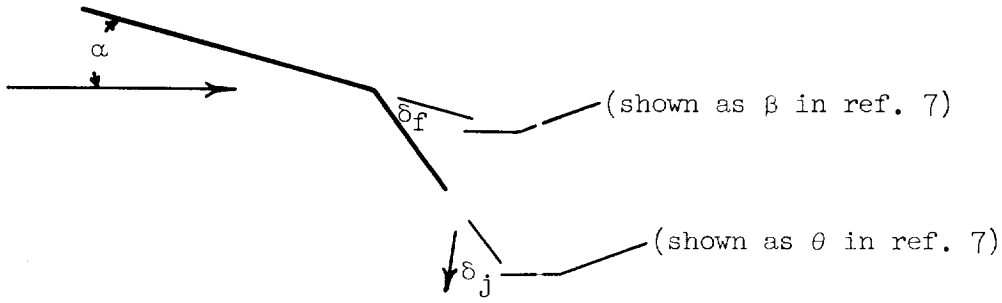

$$c_l = \alpha\left(\frac{c_l}{\alpha}\right)_{c_f/c\,=\,1} + \delta_f\left(\frac{c_l}{\delta_f}\right)_{c_f/c} + \delta_j\left(\frac{c_l}{\delta_j}\right)_{c_f/c\,=\,0}$$

Variation of c_l/α, c_l/δ_f, and c_l/δ_j with c_μ as obtained from reference 7 is presented in figure 7. For c_μ values between 0 to 1.0, variation of c_l/δ_j with c_μ (ref. 8) for blowing at the trailing edge is shown in figure 8.

The method presented in reference 9 was used to apply the above equation to a three-dimensional wing. This modification makes use of the variation of lift coefficient with flap deflection ($C_{L_{\delta_1}} = \partial C_L/\partial\delta_f$) for $c_f/c = 1$ and the effective change in two-dimensional angle of attack, $d\alpha/d\delta = (\partial c_l/\partial\delta)/(\partial c_l/\partial\alpha)$. The resulting equation for three-dimensional circulation lift consists of the sum of the following three parts:

$$\left(\frac{c_l}{\alpha}\right)_{c_f/c\,=\,1} \frac{1}{2\pi} C_{L_{\delta_1}} \frac{\alpha}{57.3} \tag{1}$$

for increment due to α. The first two components in the above expression represent $d\alpha/d\delta$.

$$\left[\frac{(c_l/\delta_f)_{c_\mu}}{(c_l/\delta_f)_{c_\mu\,=\,0}}\right]_{c_f/c} \frac{d\alpha}{d\delta} C_{L_{\delta_1}} \frac{\delta_f}{57.3} \tag{2}$$

where the first component modifies the conventional theoretical plain flap lift increment of reference 9 to allow for the increased effectiveness due to blowing.

$$\left(\frac{c_l}{\delta_j}\right)_{c_f/c = o} \frac{1}{2\pi} \frac{\underline{\delta}_j}{57.3} C_{L_{\underline{\delta}_1}} \tag{3}$$

where the first two factors are $d\alpha/d\delta$ due to the jet flap.

In addition, the lift from the jet reaction must be included. This is C_μ times the sine of jet angle. Since comparable experimental data were obtained at $\alpha_u = 0^o$, the lift increment due to α would be eliminated. The lift increment due to blowing would then be the following:

$$\Delta C_L = \left\{\left[\frac{(c_l/\delta_f)_{c_\mu}}{(c_l/\delta_f)_{c_\mu = o}}\right]_{c_f/c} \frac{d\alpha}{d\delta} C_{L_{\underline{\delta}_1}} \frac{\underline{\delta}_f}{57.3}\right\} +$$

$$\left[(c_l/\delta_j)_{c_f/c = o} \frac{1}{2\pi} \frac{\underline{\delta}_j}{57.3} C_{L_{\underline{\delta}_1}}\right] + (C_\mu \sin \underline{\delta}_j) \tag{4}$$

For the jet flap, the first term of the above equation would be eliminated.

The following values were used to calculate jet flap effectiveness for the subject wing:

$C_{L_{\underline{\delta}_1}}$ 1.44 (from cross plot of fig. 5, ref 9)

$d\alpha/d\delta$ 0.58 (from curve for theoretical plain flap effectiveness, fig. 3, ref. 9; average plain flap chord ratio of 0.23 perpendicular to flap hinge line)

$\underline{\delta}_f$ $\tan^{-1}(\cos \Lambda_f \tan \delta_f) = \tan^{-1}(0.895 \tan \delta_f)$

$\underline{\delta}_j$ $\tan^{-1}(0.895 \tan \delta_j)$

Values of c_l/α, c_l/δ_f, and c_l/δ_j were obtained from figures 7 and 8, and the conversion from c_μ to C_μ was obtained by the relationship (from ref. 1)

$$C_\mu = c_\mu \frac{S_f}{S} \cos^2 \Lambda_f$$

REFERENCES

1. Kelly, Mark W., and Tolhurst, William H., Jr.: Full-Scale Wind-Tunnel Tests of a 35° Sweptback-Wing Airplane With High-Velocity Blowing Over the Trailing-Edge Flaps. NACA RM A55I09, 1955.

2. Kelly, Mark W., and Tucker, Jeffrey H.: Wind-Tunnel Tests of Blowing Boundary-Layer Control With Jet Pressure Ratios Up to 9.5 on the Trailing-Edge Flaps of a 35° Sweptback-Wing Airplane. NACA RM A56G19, 1956.

3. Dimmock, N. A.: An Experimental Introduction to the Jet Flap. NGTE Report R. 175, Brit. Ministry of Supply, July 1955. (Also available as NGTE M. 255, May 1955 and British MOS C.P. 344)

4. Jousserandot, P.: Summary of the Systematic Tests of Supercirculation by Blowing at the Trailing Edge of a Profile in Incompressible Flow. David W. Taylor Model Basin Aero Rep. 881, Washington, July 1955.

5. Chaplin, H. R.: Preliminary Investigation of a Jet-Flap Wing Configuration. David W. Taylor Model Basin Aero Rep. 896, Washington, April 1956.

6. Lockwood, Vernard E., Turner, Thomas R., and Riebe, John M.: Wind-Tunnel Investigation of Jet-Augmented Flaps on a Rectangular Wing to High Momentum Coefficients. NACA TN 3865, 1956.

7. Malavard, Lucien C.: Recent Developments in the Method of the Rheoelectric Analogy Applied to Aerodynamics. Jour. Aero. Sci., vol. 24, no. 5, May 1957, pp. 321-331. (Also available as IAS preprint 699, 1957)

8. Poisson-Quinton, Ph., and Jousserandot, P.: High Lift and Control of Airplanes by Circulation Control. Trans. by G. Boehler, ONERA, July 1955. (Also available as Eng. Study 186, School of Eng., Wichita Univ.)

9. DeYoung, John: Theoretical Symmetric Span Loading Due to Flap Deflection for Wings of Arbitrary Plan Form at Subsonic Speeds. NACA Rep. 1071, 1952. (Supersedes NACA TN 2278)

TABLE I.- COORDINATES OF THE WING AIRFOIL SECTIONS NORMAL TO THE WING QUARTER-CHORD LINE AT TWO SPAN STATIONS
(Dimensions given in inches)

Section at 0.491 semispan			Section at 0.863 semispan		
x	z		x	z	
	Upper surface	Lower surface		Upper surface	Lower surface
0	0.231	- - -	0	-0.098	- - -
.119	.728	-0.307	.089	.278	-0.464
.239	.943	-.516	.177	.420	-.605
.398	1.127	-.698	.295	.562	-.739
.597	1.320	-.895	.443	.701	-.879
.996	1.607	-1.196	.738	.908	-1.089
1.992	2.104	-1.703	1.476	1.273	-1.437
3.984	2.715	-2.358	2.952	1.730	-1.878
5.976	3.121	-2.811	4.428	2.046	-2.176
7.968	3.428	-3.161	5.903	2.290	-2.401
11.952	3.863	-3.687	8.855	2.648	-2.722
15.936	4.157	-4.064	11.806	2.911	-2.944
19.920	4.357	-4.364	14.758	3.104	-3.102
23.904	4.480	-4.573	17.710	3.244	-3.200
27.888	4.533	-4.719	20.661	3.333	-3.250
31.872	4.525	-4.800	23.613	3.380	-3.256
35.856	4.444	-4.812	26.564	3.373	-3.213
39.840	4.299	-4.758	29.516	3.322	-3.126
43.825	4.081	-4.638	32.467	3.219	-2.989
47.809	3.808	-4.452	35.419	3.074	-2.803
51.793	3.470	-4.202	38.370	2.885	-2.574
55.777	3.066	-3.891	41.322	2.650	-2.302
59.761	2.603	-3.521	42.273	2.374	-1.986
[a]63.745	2.079	-3.089	[a]47.225	2.054	-1.625
83.681	-.740	- - -	63.031	.321	- - -
Leading-edge radius: 1.202, center at (1.201, 0.216)			Leading-edge radius: 0.822, center at (0.822, -0.093)		

[a]Straight lines to trailing edge

A-21242

Figure 1.- Photograph of the model in the Ames 40- by 80-foot wind tunnel.

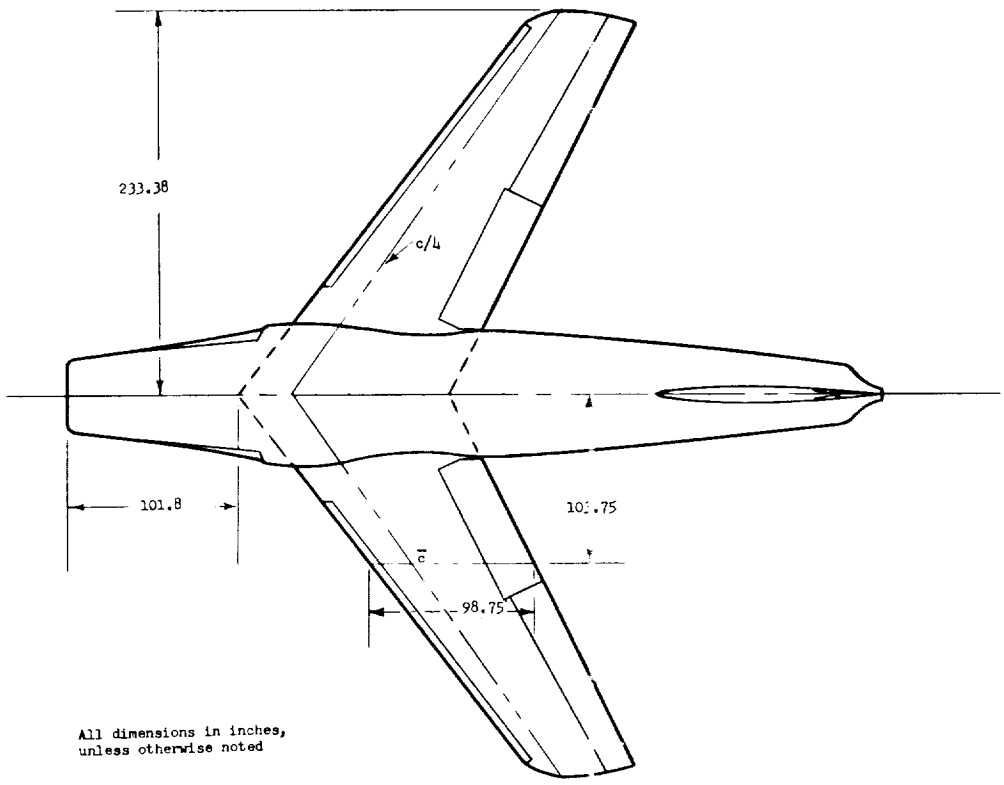

Wing	
Sweep (quarter-chord line)	35.00°
Aspect ratio	4.94
Taper ratio	0.50
Twist	2.0°
Dihedral	1.0°
Area	306.10 sq ft
Incidence (root)	1.0°
Airfoil section (root)	NACA 0012-64 (modified)
Airfoil section (tip)	NACA 0011-64 (modified)
Ratio of wing area spanned by flaps to total wing area (S_f/S)	0.367

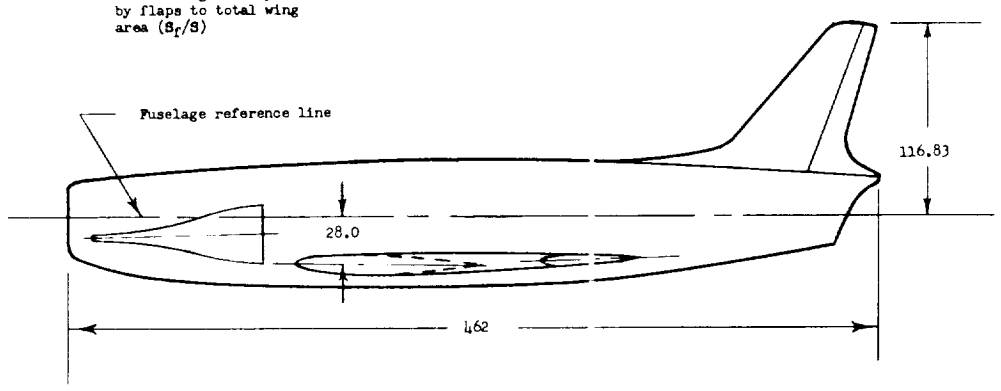

Figure 2.- General arrangement of model.

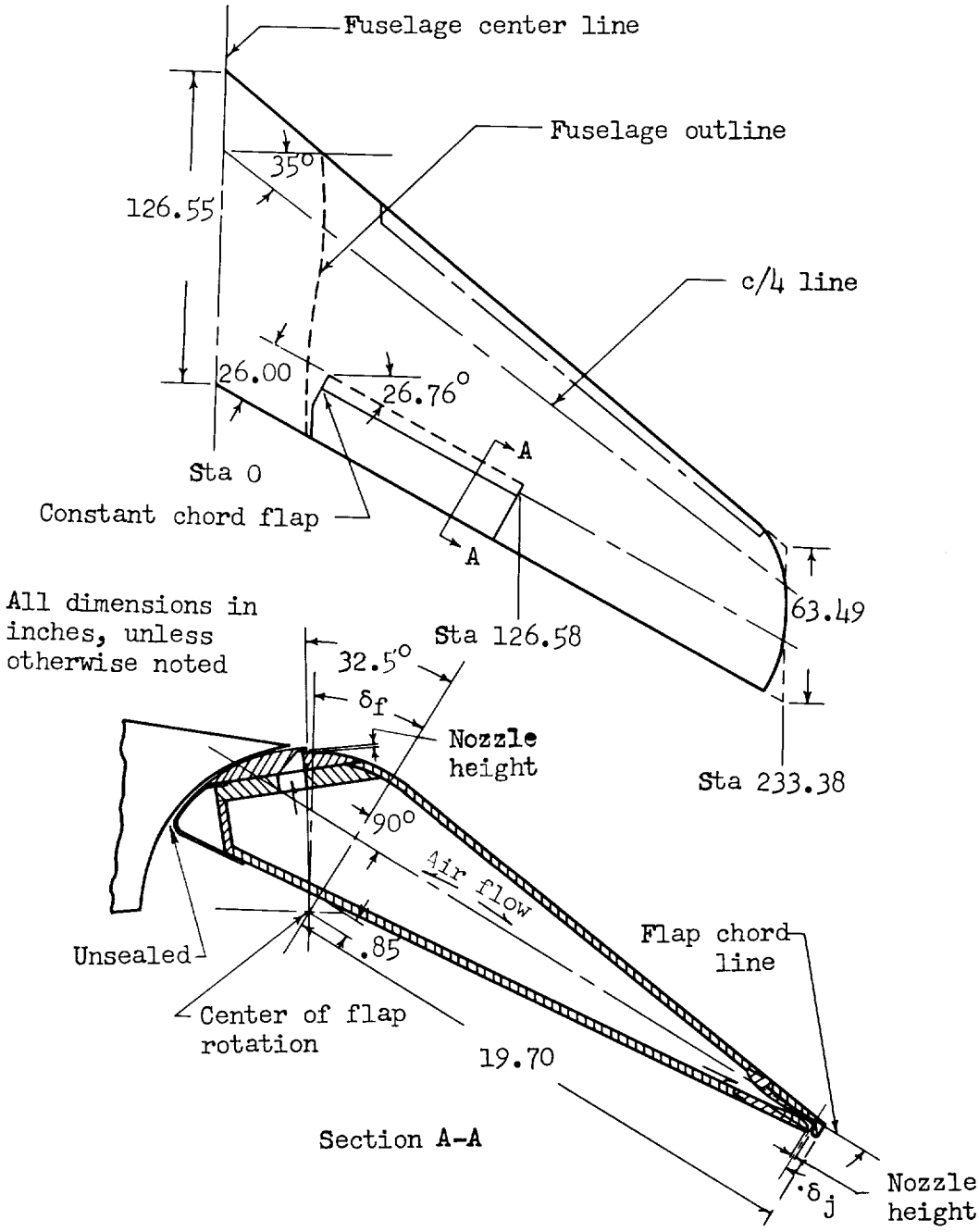

Figure 3.- Details of wing and blowing nozzle arrangements.

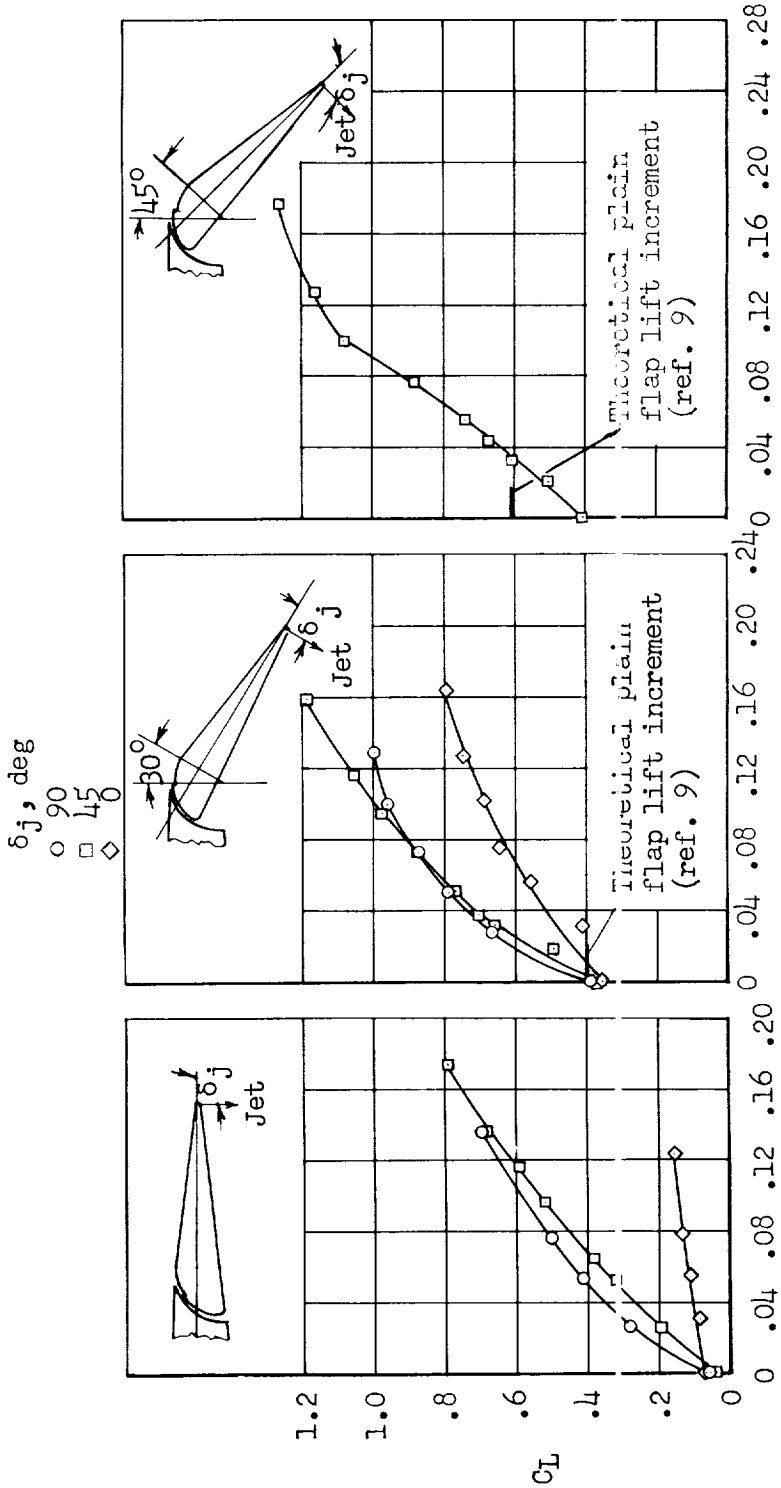

(a) Jet flap without BLC at the plain flap radius.

Figure 4.- Variation of C_L with C_μ with the jet flap with and without boundary-layer control over the plain flap radius; $\alpha_\mu = 0^\circ$.

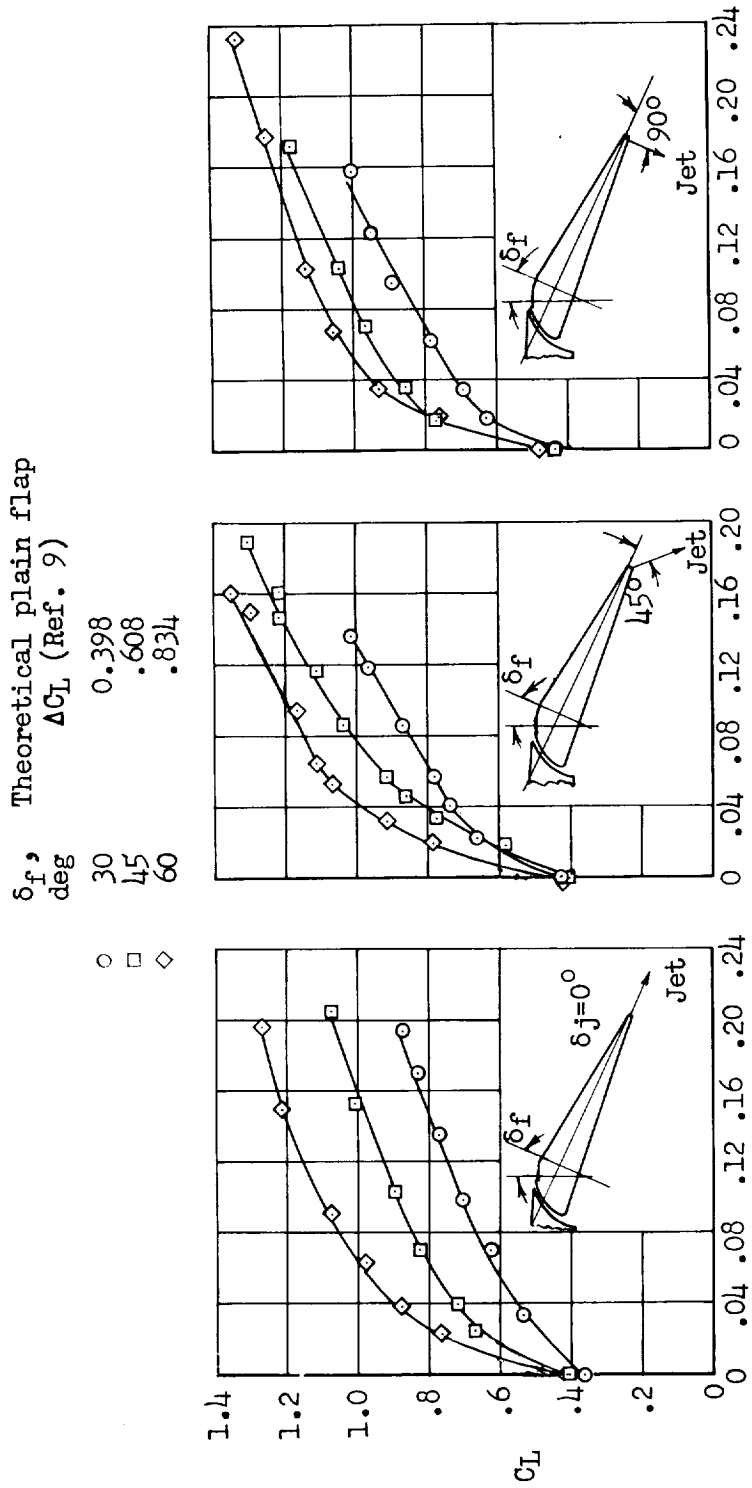

(b) Jet flap with BLC at the plain flap radius.

Figure 4.- Continued.

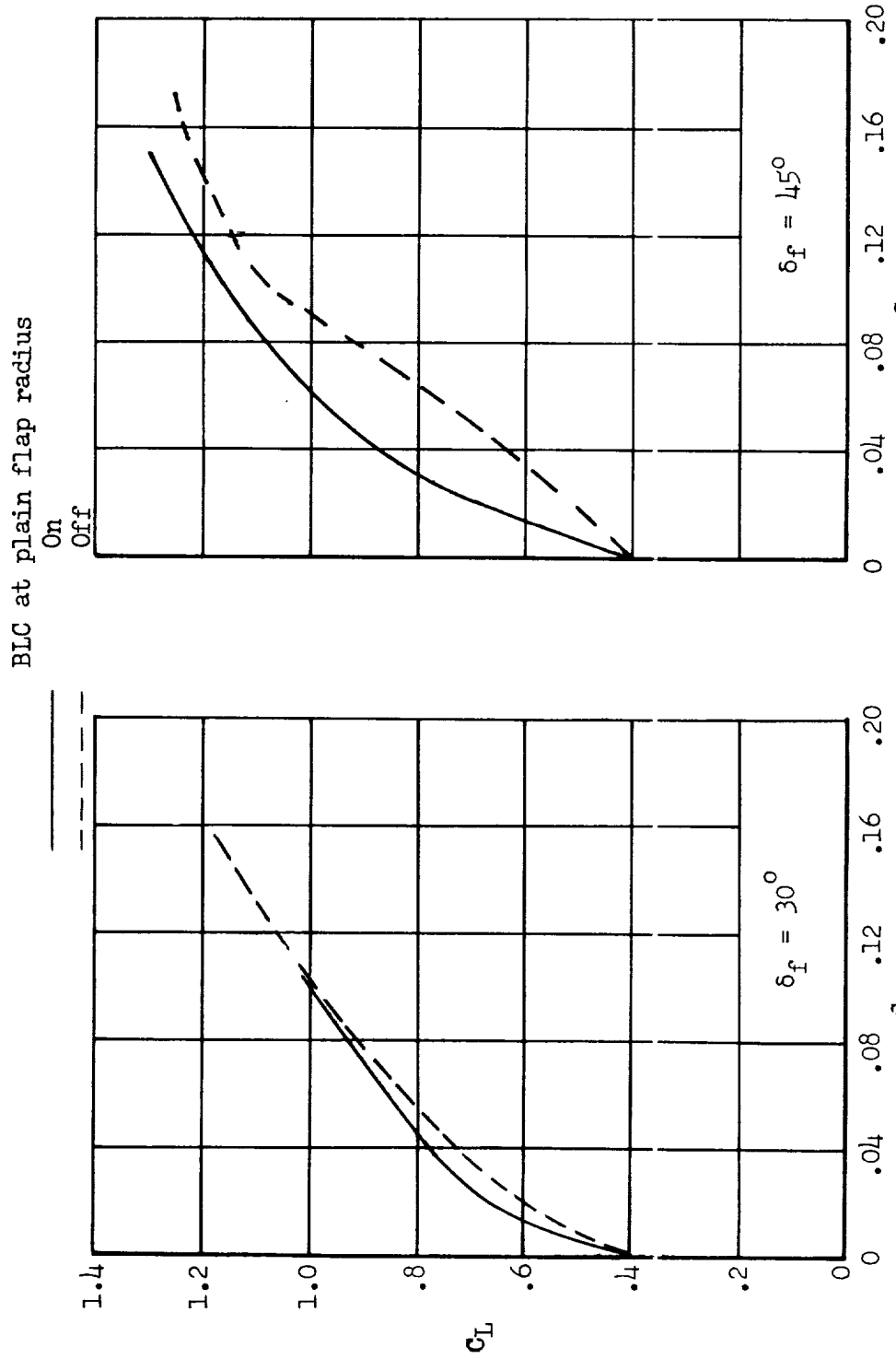

(c) Effect of BLC at the plain flap radius combined with the jet flap; $\delta_j = 45^\circ$.

Figure 4.- Continued.

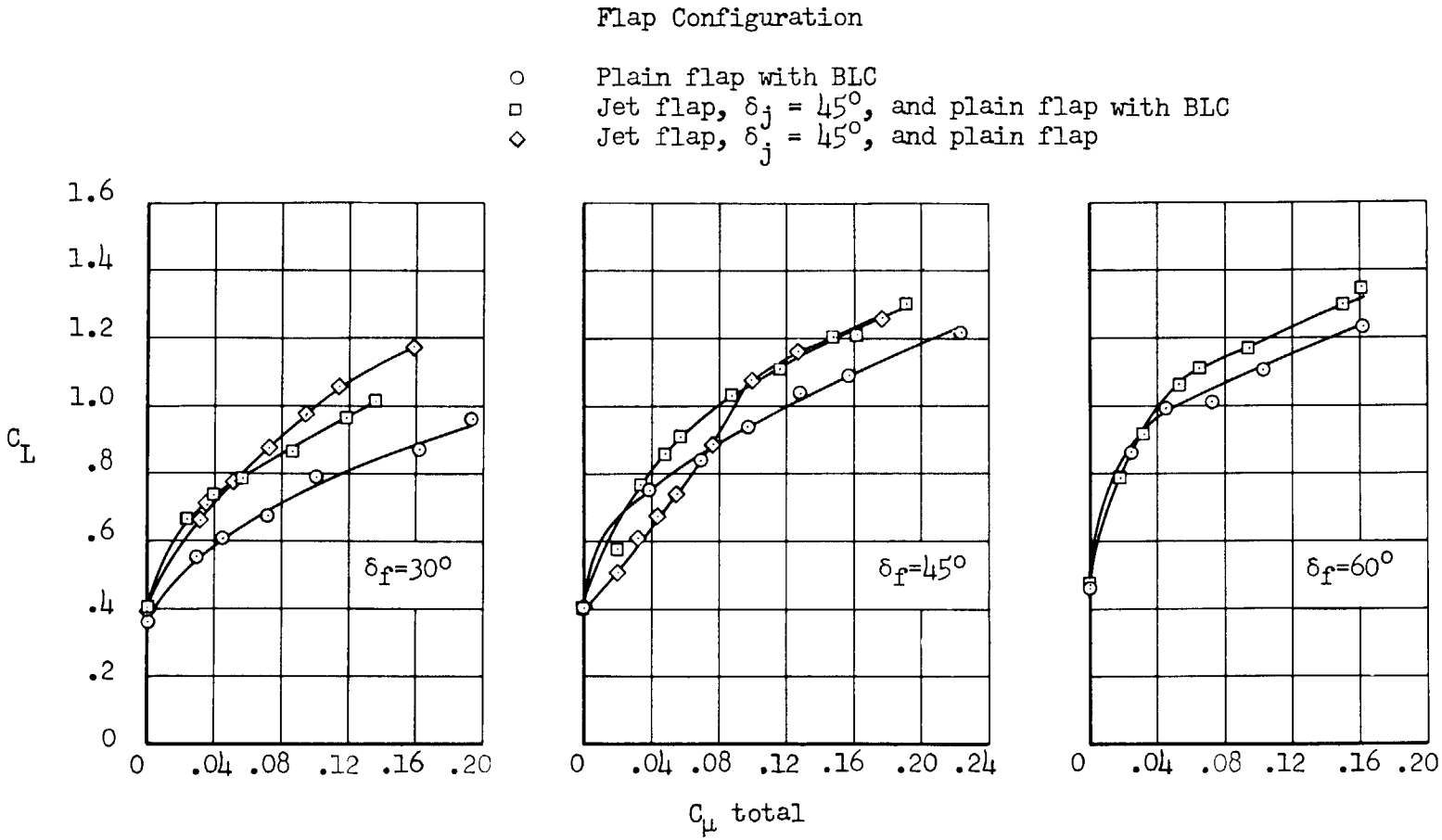

(d) Comparison of lift with C_μ between BLC plain flap and the jet flap combined with the plain flap with and without BLC.

Figure 4.- Concluded.

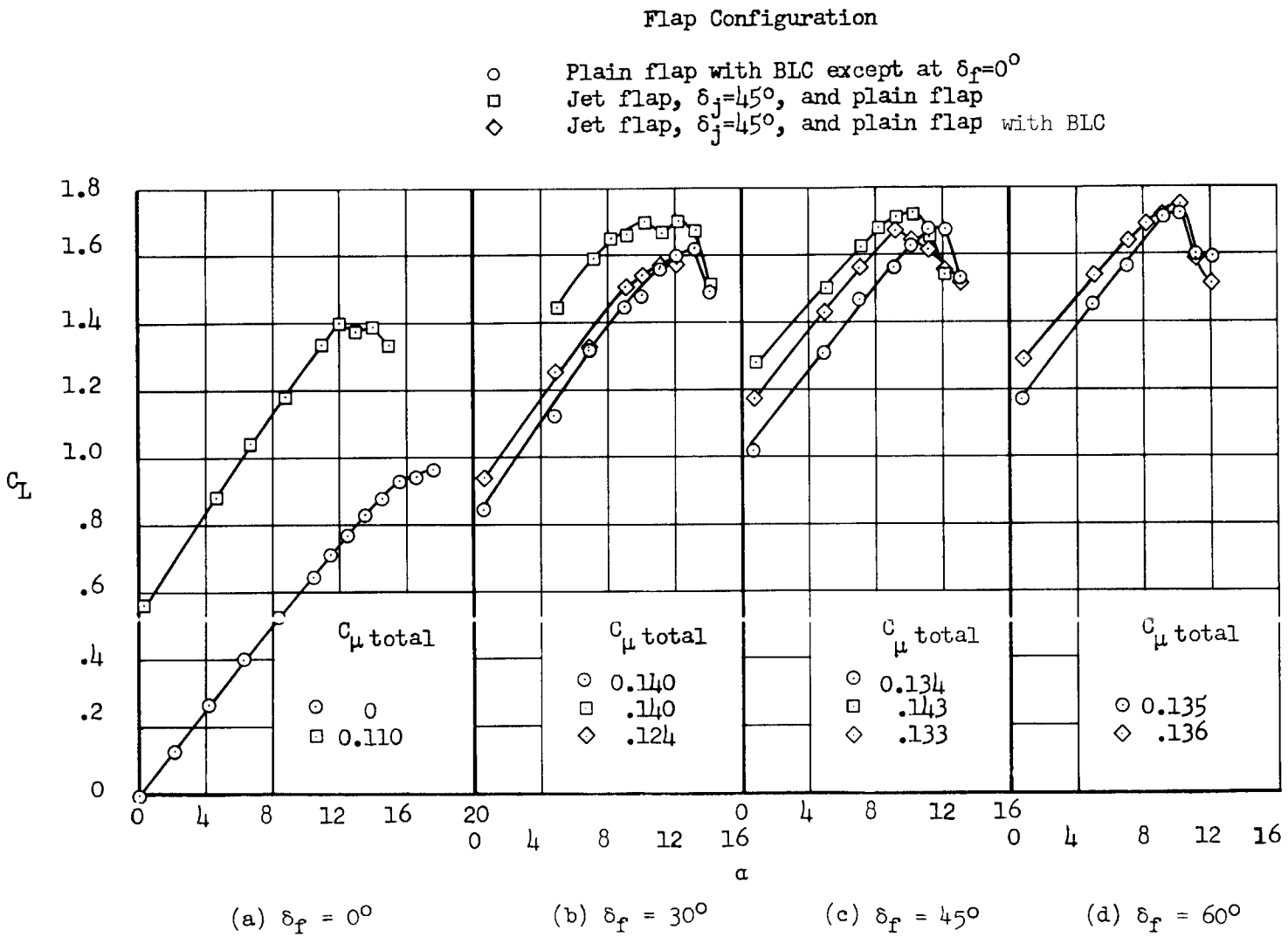

Figure 5.- Typical variation of C_L with α with various combinations of jet flap and plain flap with and without BLC.

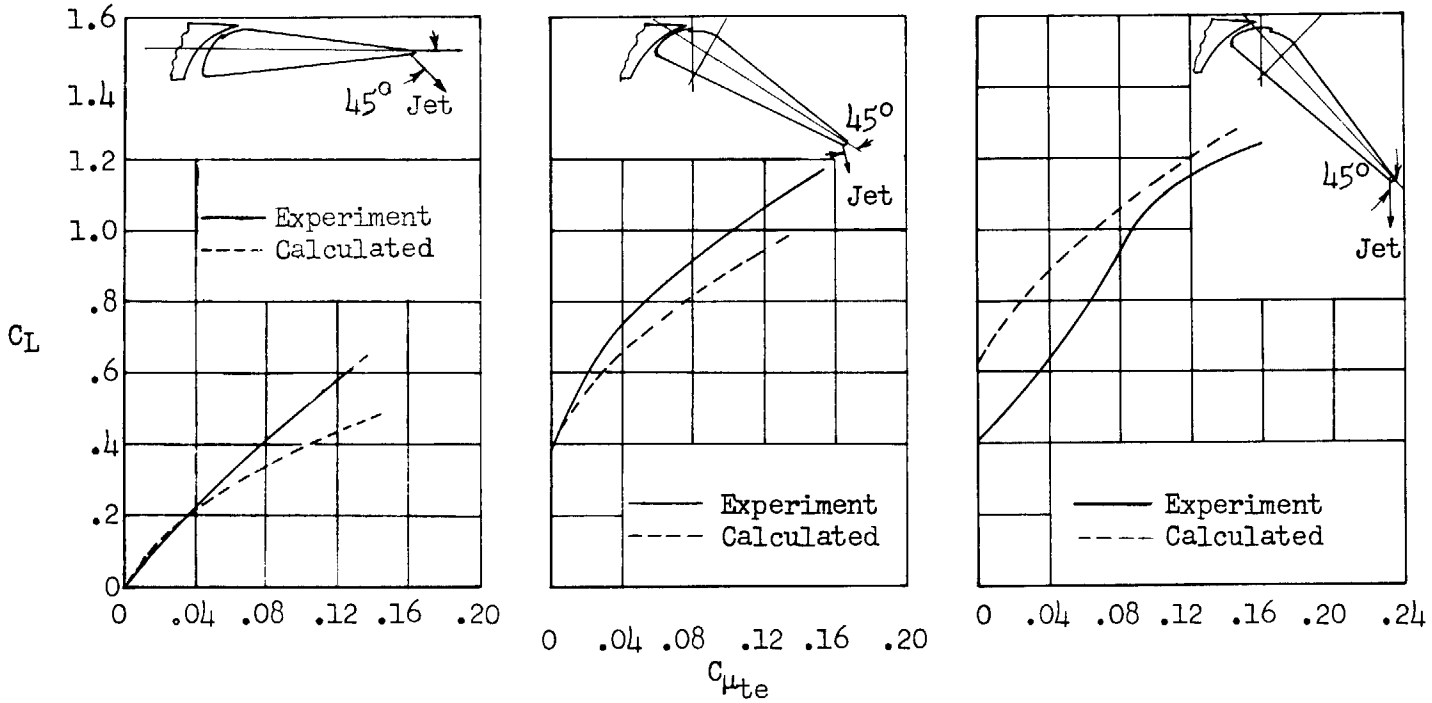

(a) $\delta_f = 0^\circ$ (b) $\delta_f = 30^\circ$ (c) $\delta_f = 45^\circ$

Figure 6.- Comparison of jet flap effectiveness between experimental data and calculated results, using the theoretical investigations of references 7 and 9; $\alpha_u = 0^\circ$.

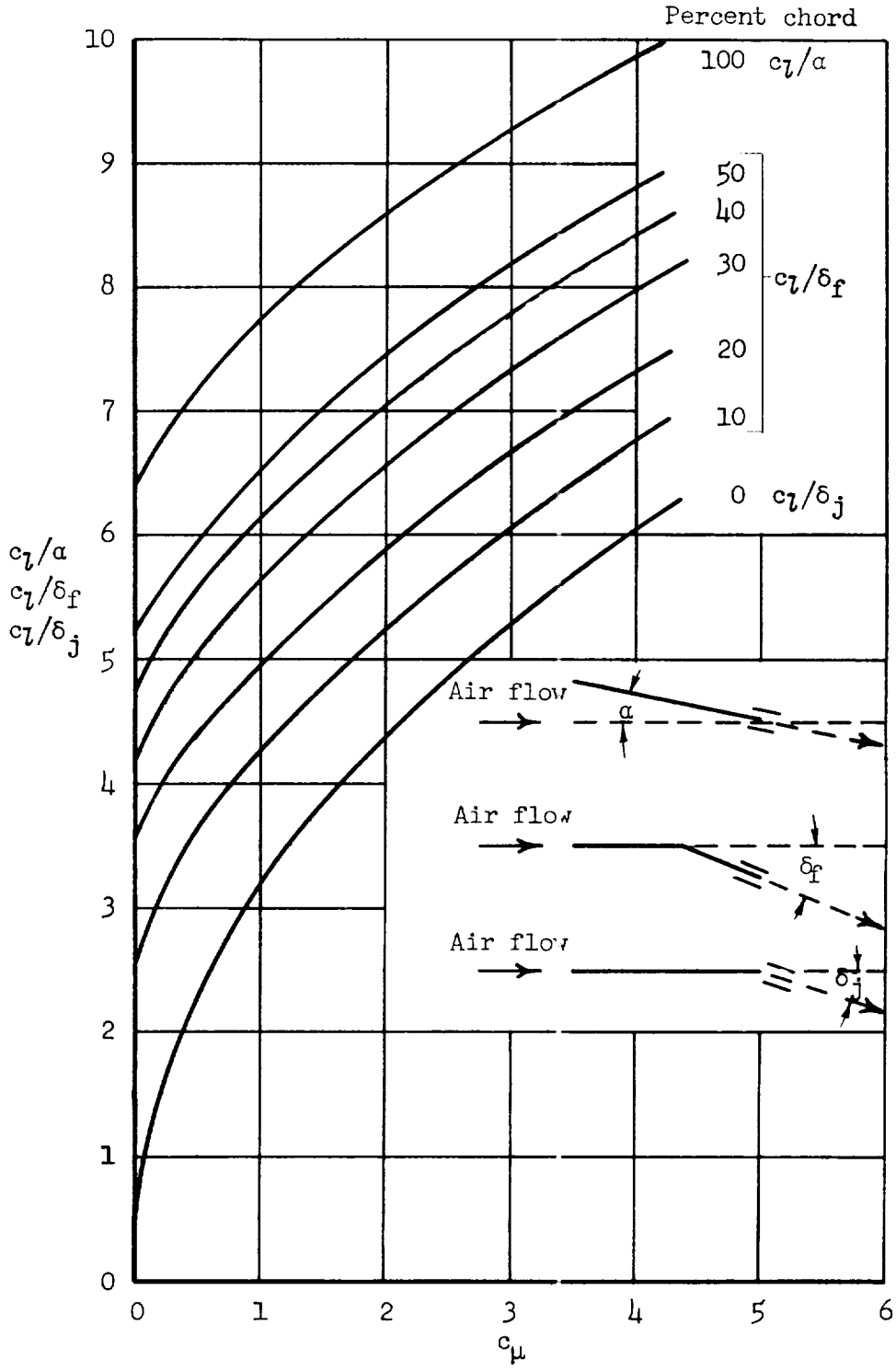

Figure 7.- Variation of c_l/α, c_l/δ_f, and c_l/δ_j, with c_μ obtained from reference 7.

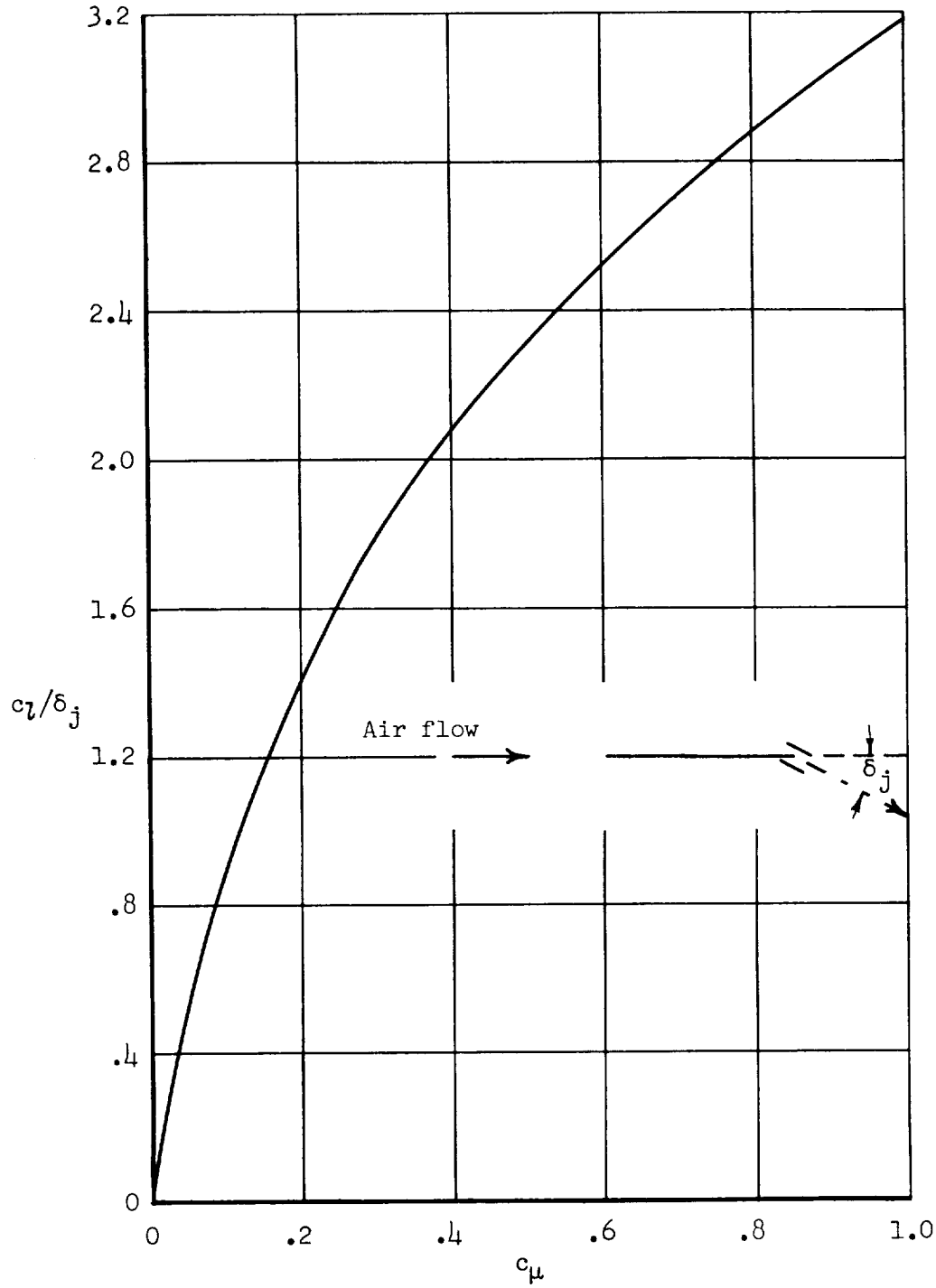

Figure 8.- Variation of c_l/δ_j with c_μ obtained from reference 8.

NASA - Langley Field, Va. A-147